Pb-ruthenate interlayer due to intermixing at high temperatures reduces the compositional gradient between the electrode and the ferroelectric and thereby the tendency for defect migration is less. In effect, $RuO_2$ electrodes in PZT thin film capacitors reduce the tendency for defect migration and entrapment at the interface that may result in structural damage to the interface and eventual loss of polarization.

Higher dc leakage current levels were observed in PZT films on Pt electrodes when compared to $RuO_2$ electrodes. Films on $RuO_2$ electrodes also showed better TDDB characteristics under an ac field. Improvement in degradation properties were observed with decreasing thickness of the films. The reason for this observation is attributed to the better adhesion of the thinner films on the bottom electrode.

## Acknowledgment

This work was supported in part by DARPA through a project from ONR. This work was supported also by Center for Advanced Ceramic Materials, The Virginia Center for Innovative Technology. The authors thank Dr. I. K. Yoo, Dr. C. K. Kwok, Dr. N. R. Parikh, and Mr. E. A. Hill for their useful contributions.

Manuscript submitted Jan. 6, 1993; revised manuscript received April 1, 1993.

*The Virginia Polytechnic Institute and State University assisted in meeting the publication costs of this article.*

REFERENCES

1. D. W. Chapman, *J. Appl. Phys.*, **40,** 2381 (1969).
2. R. B. Atkin, *Ferroelectrics,* **3,** 213 (1972).
3. T. Nakagawa, J. Yamaguchi, T. Usuki, Y. Matsui, M. Okuyama, and Y. Hamakawa, *Jpn, J. Appl. Phys.*, **18,** 897 (1979).
4. M. Sayer, *Proceedings of the Sixth Symposium on Applied Ferroelectricity*, p. 559, *IEEE,* New York (1986).
5. J. T. Evance and R. Wormack, *IEEE J. Solid State Circuits,* **23,** 1171 (1988).
6. J. F. Scott and C. A. Paz De Araujo, *Science,* **246,** 1400 (1989).
7. A. Tasch and L. Parker, Proc. *IEEE,* **77,** 374 (1989).
8. D. B. Fraser and J. R. Maldonado, *J. Appl. Phys.*, **41,** 2172 (1970).
9. I. S. Zheludev, *Physics of Crystalline Dielectrics, Electrical Properties,* Vol. 2, p. 474, Plenum, New York (1971).
10. A. Y. Kudzin, T. U. Panchenko, and S. P. Yudin, *Sov. Phys. Solid State,* **16,** 1589 (1975).
11. G. Rohrer, S. Narayan, L. McMillan, and A. Kulkarni, *J. Vac. Sci. Technol. A,* **6,** 1756 (1988).
12. H. M. Duiker, P. D. Beale, and J. F. Scott, *Bull. Am. Phys. Soc.*, **33,** 539 (1988).
13. I. K. Yoo and S. B. Desu, *Mater. Sci. Eng.*, **B13,** 319 (1992).
14. N. R. Parikh, J. T. Stephen, M. L. Swanson, and E. A. Myers, *Mat. Res. Soc. Symp. Proc.*, **200,** 193 (1990).
15. L. Krusin-Elbaum and M. Whittmer, *This Journal,* **135,** 2610 (1988).
16. M. L. Green, M. E. Gross, L. E. Kappa, K. J. Schnoes, and D. Barsen, *ibid.*, **132,** 2677 (1985).
17. S. Saito and K. Kuramasu, *Jpn. J. Appl. Phys.*, **31,** 135 (1992).
18. G. Yi and M. Sayer, *Ceram. Bull.*, **70,** 1173 (1991).
19. R. D. Standley and U. Ramaswamy, *J. Appl. Phys.*, **46,** 4887 (1975).
20. S. B. Desu and C. K. Kwok, *Mat. Res. Soc. Symp. Proc.*, **200,** 267 (1990).
21. J. M. Longo, P. M. Raccah and J. B. Goodenough, *Mat. Res. Bull.*, **4,** 191 (1969).
22. Anonymous, *Microprocessors and Microsystems,* **13,** 291 (1989).
23. J. F. Scott, C. A. Araujo, B. M. Melnick, L. D. McMillan, and R. Zuleeg, *J. Appl. Phys.*, **70,** 383 (1991).

# Characterization of Semi-Insulating Polycrystalline Silicon Prepared by Low Pressure Chemical Vapor Deposition

**Tien Sheng Chao**

*National Nano Devices Laboratory, Hsinchu 300, Taiwan, China*

**Chung Len Lee* and Tan Fu Lei**

*Department of Electronics Engineering and Institute of Electronics, National Chiao Tung University, Taiwan, China*

ABSTRACT

We employed the multiple angle incident ellipsometer to study the growth mechanism and optical properties of semi-insulating polycrystalline silicon (SIPOS) films deposited by the low-pressure chemical vapor deposition (LPCVD) technique. A significant difference of the imaginary part of the refractive index between film at the edge and those in the central region of the wafer was observed. Our analyses showed that it was consistent with the $N_2O$ depletion model. This $N_2O$ depletion phenomenon was confirmed by Auger analysis. Moreover, we found that spatial $N_2O$ depletion at the edge of the wafer was greatly influenced by the flow rate of $SiH_4$ to $N_2O$ gases. Excessively high $N_2O$ flow rate suppressed the silicon microcrystal formation, resulting in a thinner SIPOS film.

Semi-insulating polycrystalline silicon (SIPOS) has been used as a passivation material to replace oxide in high voltage semiconductor devices.[1-3] This replacement is because oxide films fail to overcome three challenging problems to meet the requirements of modern integrated-circuit planar technology; (*i*) the existence of fixed charges, usually positive ions, in oxide films. These fixed charges induce and accumulate electrons near the silicon/oxide interface, which makes it difficult to produce a high voltage planar transistor;[4] (*ii*) oxide films are not able to keep the accumulated electron charges or ionic contaminations, such as sodium, from the passivation layer;[5,6] (*iii*) the hot carrier, once injected into oxide, stays long in it resulting in a walk-out phenomenon of breakdown voltage in the p-n junction. These three problems lead to charges trapped in oxide films and subsequent inducement of charges[7] of opposite polarity near the surface. Therefore, the stability and reliability of the circuit passivation by oxide films are not achievable in high voltage semiconductor devices.

In contrast to oxide, SIPOS films are semi-insulating and almost neutral for its deep level centers pinning the Fermi-level near midgap.[8,9] Therefore, SIPOS can be used for sur-

* Electrochemical Society Active Member.

Downloaded on 2014-04-28 to IP 140.113.38.11 address. Redistribution subject to ECS terms of use (see ecsdl.org/site/terms_use) unless CC License in place (see abstract).

face passivation on both p- and n-type silicon. When a silicon surface is passivated by SIPOS, the contaminating ions drift into the passivation layer. Momentarily, the induced opposite polarity charges either neutralize the charges or form a space-charge region within the SIPOS layer. Consequently, a shielding effect in the silicon surface region is achieved, and this copes with the problem of the injected hot carrier at high fields.

SIPOS film usually has been deposited by low-pressure chemical vapor deposition (LPCVD) technique using mixture of silane ($SiH_4$) and nitrous oxide ($N_2O$) at 650°C.[10] This material has been reported as an excellent passivation film for high voltage transistors[1,2,11] and carrier injector in electrically erasable and programmable read-only memories (EEPROMs).[12] It, instead of polysilicon, was used also as an emitter because of its larger band gap, which offers better minority carrier blocking properties than that of the conventional diffused emitter.[13] The chemical composition of SIPOS is $SiO_x$, where $x$ ranges from 0.48 to less than 2, and the oxygen concentration increased with the partial pressure of $N_2O$. From the results of transmission electron microscopic (TEM) analysis, Hamasaki *et al.*[3] found that the SIPOS consisted of silicon microcrystals, silicon oxide, and disordered silicon. The size of silicon microcrystals in SIPOS decreased as the oxygen concentration increased, *i.e.*, increasing the partial pressure of $N_2O$.

Multiple angle incident (MAI) ellipsometry measurement, for its high sensitivity and nondestructiveness, has been used in many fields. It has been applied to characterize the optical coating,[14] the oxygen-ion-implanted silicon-on-insulator (SOI),[15] multiple-layer heterostructure.[16] MAI ellipsometry is used here to study the growth mechanism and optical properties of SIPOS. The Auger analysis was employed to characterize the oxygen concentration in the SIPOS film.

## Experimental

Silicon wafers, n-type (100), 4-5 Ω-cm, were used and cleaned by the RCA process. Wafers then were dipped in buffered HF solution followed by a DI water rinse. Subsequently, a $SiO_2$ film of 220Å thickness was grown on those wafers in a dry oxygen ambient at 1000°C for 17 min. The samples then were put into an LPCVD system to deposit SIPOS films. Different flow rate ratios of $SiH_4$ (45 sccm) to $N_2O$ (10, 15, 20, 30, and 35 sccm) were used to deposit the SIPOS film at 650°C for 30 min. Samples were measured by MAI ellipsometry with the incident angles varying between 65 and 72 degrees at the wavelength of 632.8 nm. A sum of the least squares error fitting method was used to fit the optical constant ($\tilde{N} = N - iK$) and thickness ($T$) of SIPOS, where $N$ and $K$ are the real and the imaginary part of the refractive index $\tilde{N}$ of SIPOS, respectively. In the fitting process, a reasonable range of values of $N$, $K$, and $T$ is given. Then, the simulated values of ($\Delta$, $\psi$) can be calculated for a corresponding set of ($N$, $K$, $T$). The sum of the error of the best fit case between the measured and the simulated ellipsometric angle $\Delta$ and $\psi$ was always less than 1 degree in our measurements.

## Results and Discussion

Figure 1 shows the thickness of SIPOS films deposited with different mixing flow rates of $SiH_4$ and $N_2O$. The flow rate of $SiH_4$ was fixed at 45 sccm while the flow rate of $N_2O$ was varied between 10 and 35 sccm. As seen in Fig. 1, the thickness of SIPOS increases rapidly with $N_2O$ flow rate and then decreases monotonously as the $N_2O$ flow rate exceeds 25 sccm. Initially, as the $N_2O$ flow was varied, the partial pressure of $N_2O$ at the surface increased correspondingly, which resulted in an increase of SIPOS film thickness. However, as the flow rate of $N_2O$ exceeded 25 sccm, the wafer surface is mostly saturated with $N_2O$. This $N_2O$ saturation suppressed surface reaction on Si surface and further nucleation of Si microcrystal. Similar surface reactions were observed for the $SiH_4/O_2$ system.[17] At high oxygen concentration, the surface was merely saturated with absorbed oxygen and further deposition reaction with silane were blocked. Therefore, we conclude that the silane-oxygen reaction is dominated by gas species near the wafer surface. We also note in Fig. 1 that the SIPOS film thickness at the edge of the wafer (3 cm from the center of a 3 in. wafer) is thicker than that in the center. This depletion effect,[18] which resulted from preferential reactant gas concentration also has been observed for many conventional end-feed LPCVD systems. Deposition rates were greater on wafers near the inlet of gas than the center of the wafer. As a result, the thickness of SIPOS films at the edge of the wafer was thicker than that at the center. The top view of the wafer deposited at a $N_2O$ flow rate of 20, 25, and 30 sccm were examined also. Circular rings of various colors were evident, indicating a thickness variation across the wafer. As seen in Fig. 1, the thickness difference between the edge and the central region is minimal for $N_2O$ flow rate of either 10 or 35 sccm. Correspondingly, colorful rings were not observed on wafers with SIPOS film deposited under these conditions.

Figure 2 shows the measured real part, $N$, of the refractive index of SIPOS as a function of the $N_2O$ flow rate. For $N_2O$ flow rate less than 20 sccm, the $N$ of the wafer center region is slightly larger than that of the edge. As the flow rate of $N_2O$ exceeds 20 sccm, the $N$ value of the edge and the center reaches a same value. Figure 3 shows the measured imaginary part, $K$, of the refractive index of SIPOS *vs.* the $N_2O$ flow rate. The $K$ value decreases steadily with increasing $N_2O$ flow rate. This decrease indicates that the absorption properties of the SIPOS films decreased with increase of the oxygen concentration. For a wavelength of 632.8 nm, the silicon dioxide is almost transparent, and, hence, $K$ is zero. The absorption of the amorphous silicon is larger than single-crystalline silicon. As reported previously,[3] SIPOS films consist of Si microcrystal, disordered Si, and Si oxide. Therefore, as the oxygen concentration in the SIPOS film increases, the adsorption of the SIPOS decreases. In Fig. 3, it is clearly evident that the adsorption coefficient $K$ of the edge region is lower than that of center. This result is because the $N_2O$ gas was consumed more at the edge than in the center, resulting in a higher oxygen concentration at the edge. This result is consistent with the depletion effect observed in Fig. 1.

To further confirm the model of the $N_2O$ depletion in SIPOS film deposition, some samples were characterized by Auger analyses. A 1000Å thick thermal oxide film was analyzed and used as a standard. Figures 4 and 5 show the atomic ratio % of SIPOS film at the edge and the center of

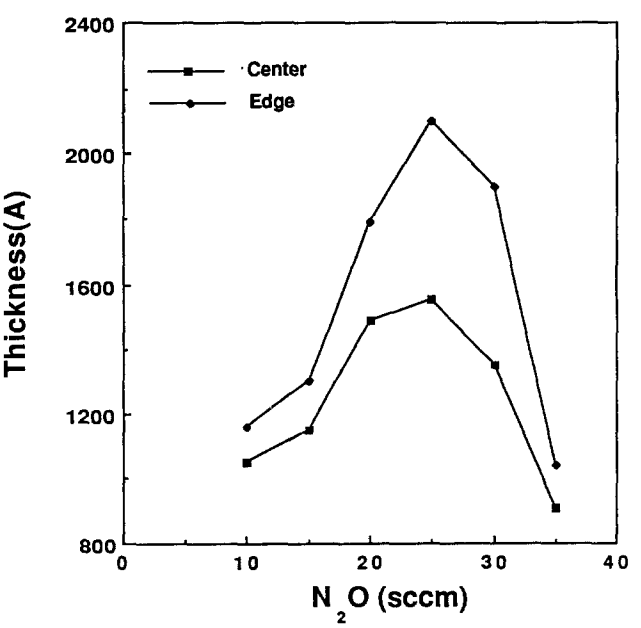


**Fig. 1. The measured thickness (Å) of SIPOS deposited in an LPCVD system at 650°C for 30 min. The flow rate of $SiH_4$ is 45 sccm and the mixing $N_2O$ flow rate is 10 to 35 sccm. The thickness of the edge is measured at a point 3 cm from center region.**

Downloaded on 2014-04-28 to IP 140.113.38.11 address. Redistribution subject to ECS terms of use (see ecsdl.org/site/terms_use) unless CC License in place (see abstract).

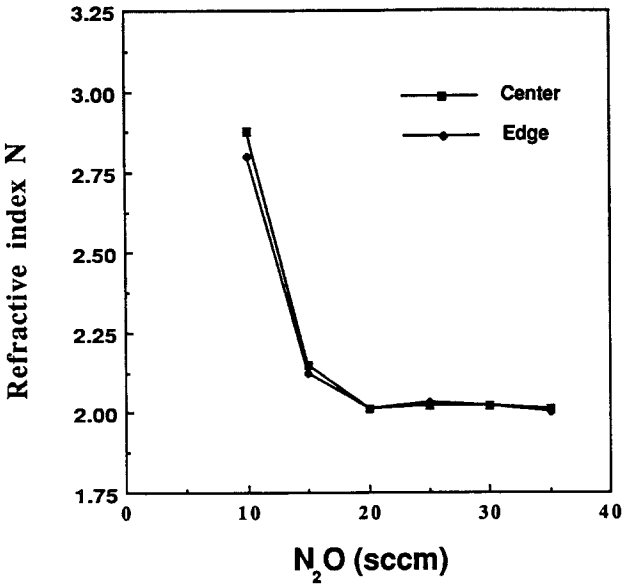


Fig. 2. The measured real part of the refractive index of SIPOS by MAI ellipsometry for 45 sccm $SiH_4$ and for different $N_2O$ flow rates changing from 10 to 35 sccm. The edge point is measured from the center at a distance of 3 cm.

a wafer, respectively. These films were deposited with 45 sccm $SiH_4$ and 25 sccm $N_2O$. The oxygen concentration at the edge of the wafer is larger than that of the center, especially near the sample surface. This confirmed our $N_2O$ depletion model as mentioned above. Figure 6 shows the atomic ratio % of Si and O of a different sample deposited with $N_2O$ flow rate of 15 sccm and a fixed $SiH_4$ flow rate of 45 sccm. The oxygen concentration is only 30% and is uniform across the entire film. From the results of Auger analysis and the ellipsometry measurement, we conclude that a uniform thickness SIPOS film is achievable with $N_2O$ flow rate less than 15 sccm. A slower flow rate of $N_2O$ also would result in a uniform SIPOS film with a constant Si/O ratio.

## Conclusion

In this work, the MAI ellipsometer was used to study the growth mechanism and optical properties of the SIPOS films grown by an LPCVD technique. For a $N_2O$ flow rate

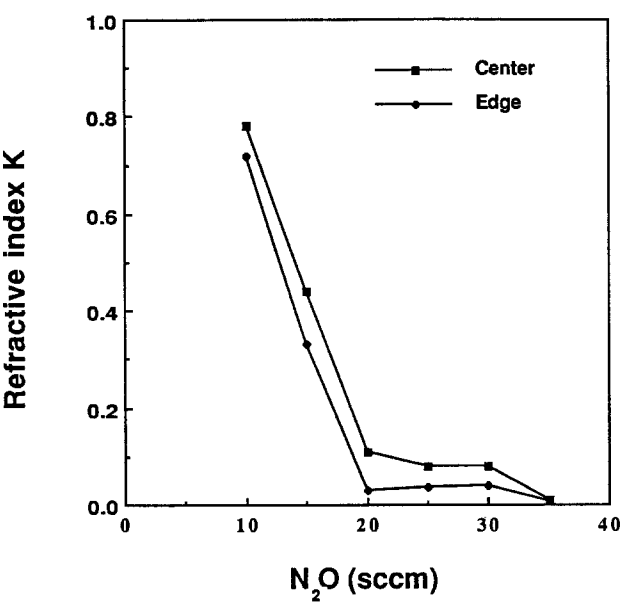


Fig. 3. The measured imaginary part of the refractive index of SIPOS by MAI ellipsometry for 45 sccm $SiH_4$ and for different $N_2O$ flow rates changing from 10 to 35 sccm. The edge point is measured from the center at a distance of 3 cm.

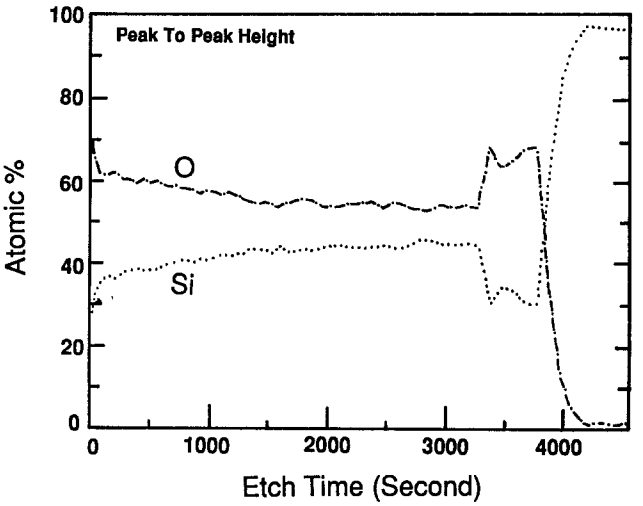


Fig. 4. Auger analysis of the atomic ratio of Si and O of the SIPOS film ($SiH_4$ : $N_2O$ = 45 : 25 sccm) at the edge of the wafer.

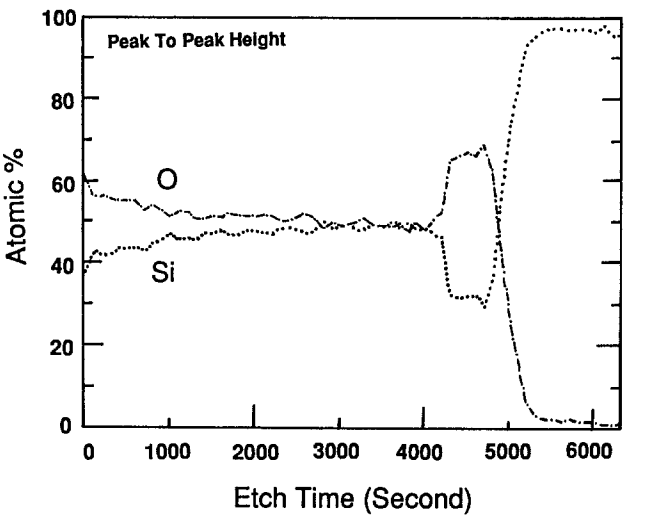


Fig. 5. Auger analysis of the atomic ratio of Si and O of the SIPOS film ($SiH_4$ : $N_2O$ = 45 : 25 sccm) at the center of the wafer.

less than 25 sccm, the thickness of the SIPOS film increased with $N_2O$ flow rate. As $N_2O$ flow rate was raised beyond 25 sccm, the existence of excessive $N_2O$ near the wafer surface, which suppressed the surface reaction for silicon mi-

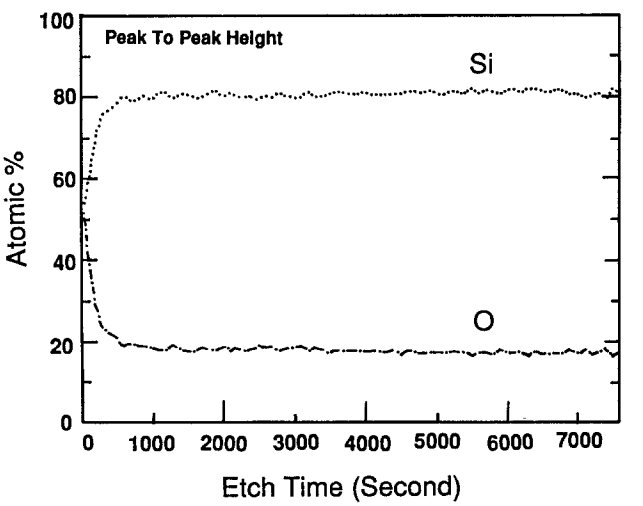


Fig. 6. Auger analysis of the atomic ratio of Si and O of the SIPOS film ($SiH_4$ : $N_2O$ = 45 : 15 sccm) at the center of the wafer.

Downloaded on 2014-04-28 to IP 140.113.38.11 address. Redistribution subject to ECS terms of use (see ecsdl.org/site/terms_use) unless CC License in place (see abstract).

crocrystal formation. The $N_2O$ depletion effect became greater for $N_2O$ flow rates in the range of 20 to 30 sccm. This depletion effect was confirmed by both Auger analyses and the ellipsometry measurement. We observed that lower flow rates resulted in a SIPOS film of better thickness uniformity and more constant Si/O ratio.

## Acknowledgment

This work is supported by the National Science Council of the Republic of China through Contract No. NSC81-4040-E009-138. The authors thank Dr. P. J. Wang for his helpful discussions.

Manuscript submitted Nov. 4, 1992; revised manuscript received May 12, 1993.

*The National Nano Devices Laboratory assisted in meeting the publication costs of this article.*

RREFERENCES

1. M. Okayama and Y. Kawana, *IEEE Trans. Electron Devices,* **ED-23,** 826 (1976).
2. A. Mimura, M. Oohayashi, S. Murakami, and N. Momma, *IEEE Electron Device Lett.,* **EDL-6,**189 (1985).
3. M. Hamasaki, T. Adachi, S. Wakayama, and M. Kikuchi, *J. Appl. Phys.,* **49,** 3987 (1978).
4. B. E. Deal, *IEEE Trans. Electron Devices,* **ED-27,** 606 (1980).
5. D. R. Kerr, J. S. Logan, P. J. Burkhardt, and W. A. Pliskin, *IBM J. Res. Dev.,* **8,** 376 (1964).
6. E. H. Nicollian and J. R. Breuws, *MOS Physics and Technology,* Wiley, New York (1982).
7. C. A. Neugebauer, *Appl. Phys. Lett.,* **19,** 287 (1971).
8. T. Aoki, T. Matsushita, H. Yamoto, H. Hayashi, M. Okuyuma, and Y. Kawana, Abstract 148, p. 352, The Electrochemical Society Extended Abstracts, Vol. 75-1, Toronto, ON, Canada, May 11-16, 1975.
9. T. Matsushita, in Seventh Conference Solid State Devices Digest Technical Papers, p. 9, Tokyo (1975).
10. W. R. Knolle and H. R. Maxwell, *This Journal,* **127,** 2254 (1980).
11. H. Hayashi, T. Mamine, and T. Matsushita, *IEEE Trans. Electron Devices,* **ED-28,** 246 (1981).
12. P. Pan, L. A. Nesbit, R. W. Douse, and R. T. Gleason, *This Journal,* **132,** 2013 (1985).
13. Y. H. Kwark and R. M. Swanson, *Solid-State Electron.,* **30,** 1121 (1987).
14. K. Memarzadeh, *J. Appl. Phys.,* **64,** 3407 (1988).
15. P. Dutta, *ibid.,* **64,** 2754 (1988).
16. P. G. Snyder, M. C. Rost, H. Bu-Abbud, and J. A. Woollam, *ibid.,* **60,** 3293 (1986).
17. C. Cobianu and C. Pavelescu, *Thin Solid Films,* **117,** 211 (1984).
18. S. Wolf and R. N. Tauber, *Silicon Processing for the VLSI Era,* Vol. 1, 170, Lattice Press, California (1986).

# Improving Metal Oxide Semiconductor Device Performance Through the Use of Ion Exchange-Purified HF

**Vikram Doshi and Lindsey Hall**

*Texas Instruments, Dallas, Texas 75265*

**Thomas Wear**

*SEMATECH, Austin, Texas 78741*

**John Davison***

*Athens Corporation, Oceanside, California 92056*

ABSTRACT

Ion-exchange purification systems were employed at two different semiconductor metal oxide semiconductor (MOS) wafer fabs to purify the dilute hydrofluoric acid solutions used in cleaning silicon wafers. One fab performed the HF cleans in immersion baths while the other fab used a spray cleaner. Both fabs observed improvements in device performance, as measured in split-lot gate oxide integrity tests, after they began using the ion exchange-purified HF. One fab also observed a significant improvement in refresh characterization time, and a 5% yield improvement at multiprobe. These improvements are believed due to the lower levels of metallic impurities in the ion exchange-purified HF. Impurity levels of over 30 elements in the treated HF are routinely below 1 ppb.

In 1989, the first hydrofluoric acid reprocessor, or HFR, was tested successfully at Texas Instruments 1 Mbit DRAM fab, DMOS IV, in Dallas, Texas.[1] The HFR used filters and ion exchangers to remove particulate and ionic impurities from dilute HF. The first HFR was designed to recycle and repurify the HF solutions used to clean furnace tubes and other quartz parts. Analysis of the reprocessed acid soon indicated that ion exchange technology had the ability to product ultrapure HF solutions.[2]

About the same time the first HFR began reprocessing the used quartz-cleaning HF in DMOS IV, the fab experienced severe problems in the wafer cleaning process. The problems were related to the purity of the dilute HF. These problems were corrected by switching to high purity HF from Japan, and implementing some process modifications. Importing HF was expensive, so, in late 1990, another HFR was installed by TI's Chemical Operations Department to manufacture high purity dilute HF solutions at low cost. The HFR proved capable of making high purity HF solutions reliably and consistently. The next step was to qualify the HF for use in the wet-clean process. The qualification took place in DMOS IV since they had a demonstrated need for high purity dilute HF. The ion exchange (IE) purified HF from the HFR was compared directly to the high purity HF from Japan then in use in a series of split-lot tests carried out simultaneously in identical wet-process hoods. No changes to the equipment, and only minor changes to the chemical distribution systems, were required. Thus, the only variable in the tests was the HF. The results of these tests indicate with a high degree of certainty that the IE purified HF gives cleaner wafer surfaces, fewer defects, and higher yields.

Also in late 1990, an HFR was installed at SEMATECH in Austin, Texas. For some time after its initial qualification,[3]

* Electrochemical Society Active Member.

Downloaded on 2014-04-28 to IP 140.113.38.11 address. Redistribution subject to ECS terms of use (see ecsdl.org/site/terms_use) unless CC License in place (see abstract).